Electronic Supplementary Information

Electrical conductivity of all-natural and biocompatible semi-interpenetrated polymer network containing a deep eutectic solvent

by

Edwin J. Gachuz, Martín Castillo-Santillán, Karla Juarez-Moreno, Jose Maya-Cornejo, Antonio Martinez-Richa, Andreu Andrio, Vicente Compañ,* Josué D. Mota-Morales*

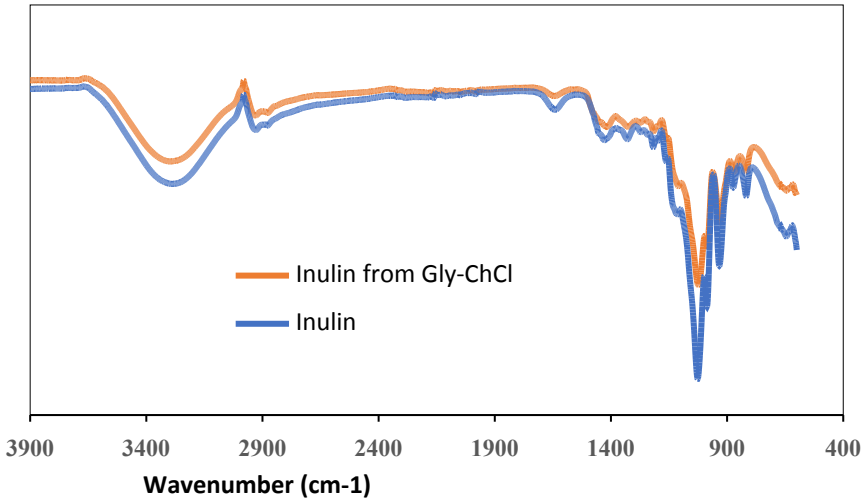

Figure S1. ATR-FTIR spectra of recovered inulin by precipitation with water after its dissolution in Gly-ChCl DES (Inulin from Gly-ChCl) compared with pure inulin.

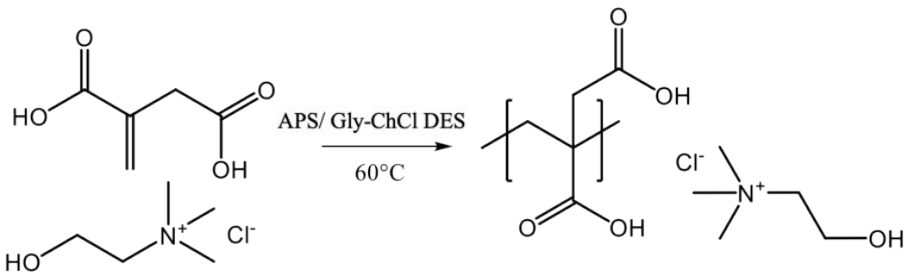

Figure S2. Scheme of free-radical polymerization/crosslinking of IA-ChCl DES in solution. (Entries 3 and 4 in Table 1).

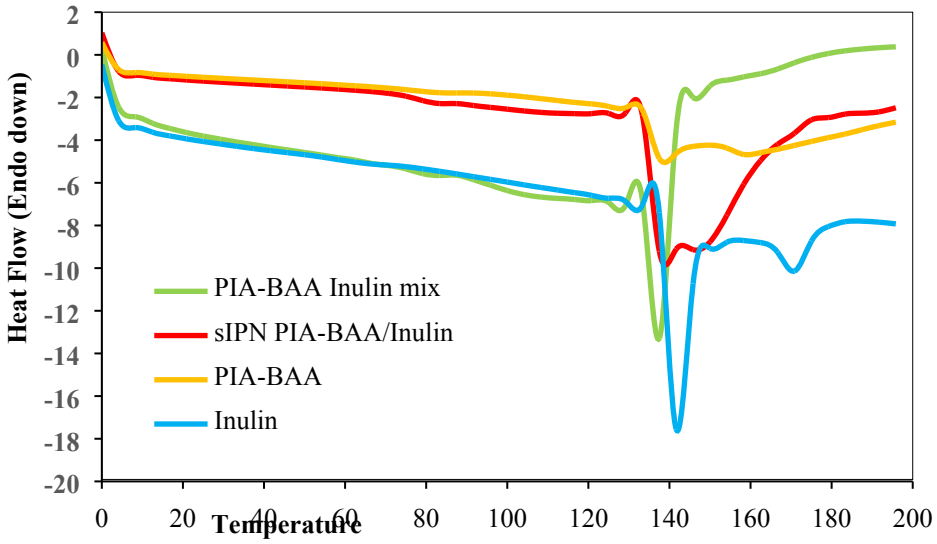

Figure S3. DSC traces of Inulin, poly(IA-co-BAA) synthesized in Gly-ChCl DES, semi-IPN poly(IA-co-BAA)/inulin, and a mixture of poly(IA-co-BAA) and inulin by swelling poly(IA-co-PETA) with an aqueous solution of inulin and subsequent lyophilization

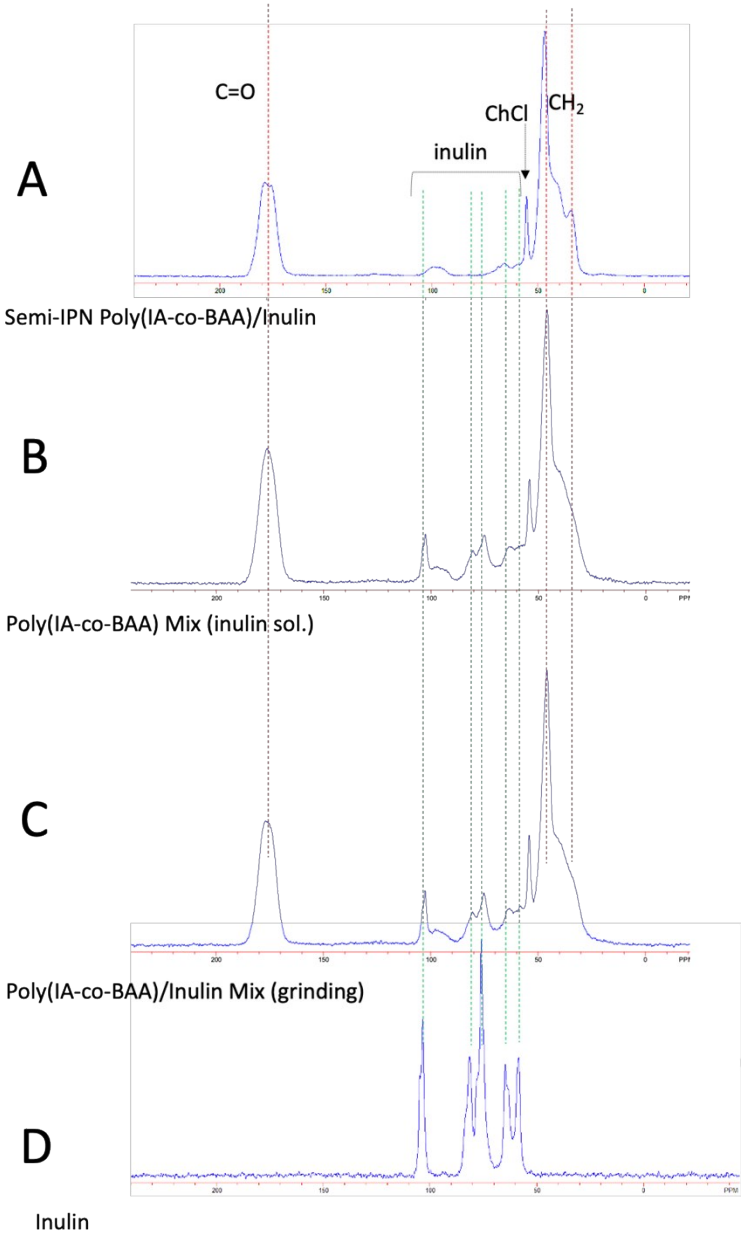

Figure S4. Solid state ^{13}C NMR spectra of A) semi-IPN poly(IA-co-BAA)/inulin; D) inulin, and mixtures of poly(IA-co-BAA) and inulin by: B) swelling poly(IA-co-PETA) with an aqueous solution of inulin and subsequent lyophilization, and B) grinding.

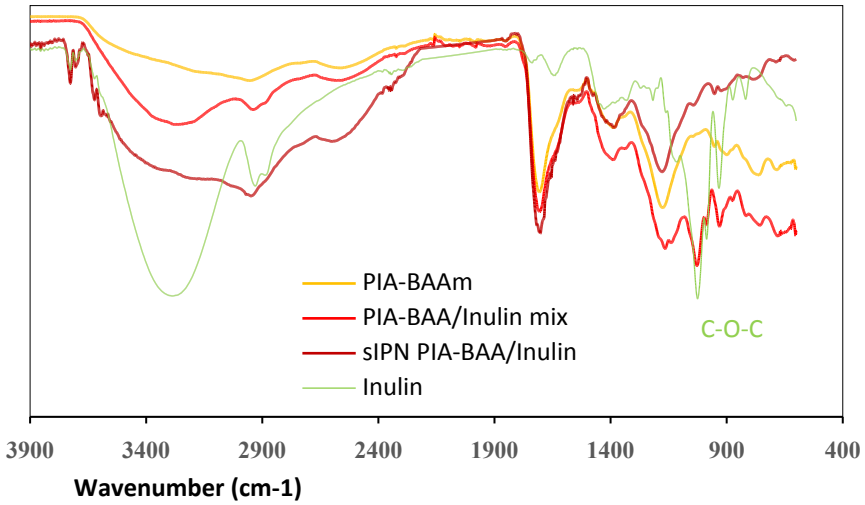

Figure S5. ATR-FTIR spectra of Inulin, poly(IA-co-BAA) synthesized in Gly-ChCl DES, semi-IPN poly(IA-co-BAA)/inulin, and a mixture of poly(IA-co-BAA) and inulin by swelling poly(IA-co-PETA) with an aqueous solution of inulin and subsequent lyophilization

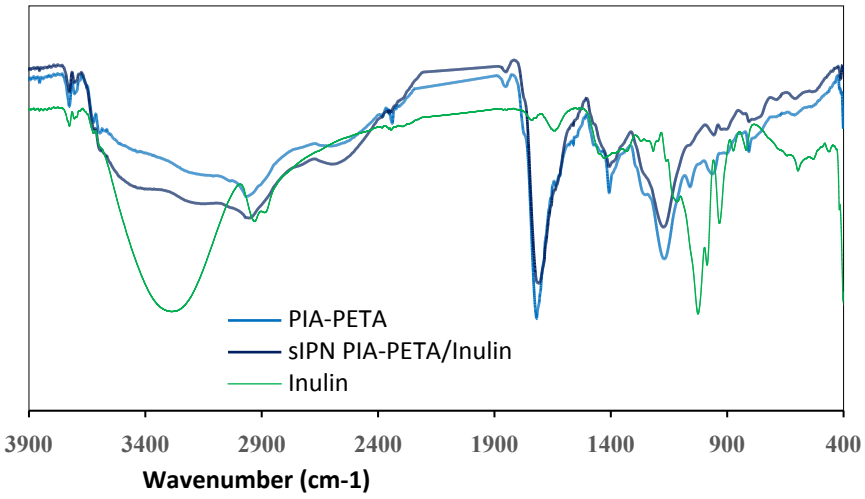

Figure S6. ATR-FTIR spectra of Inulin, semi-IPN poly(IA-co-PETA)/inulin and poly(IA-co-PETA).

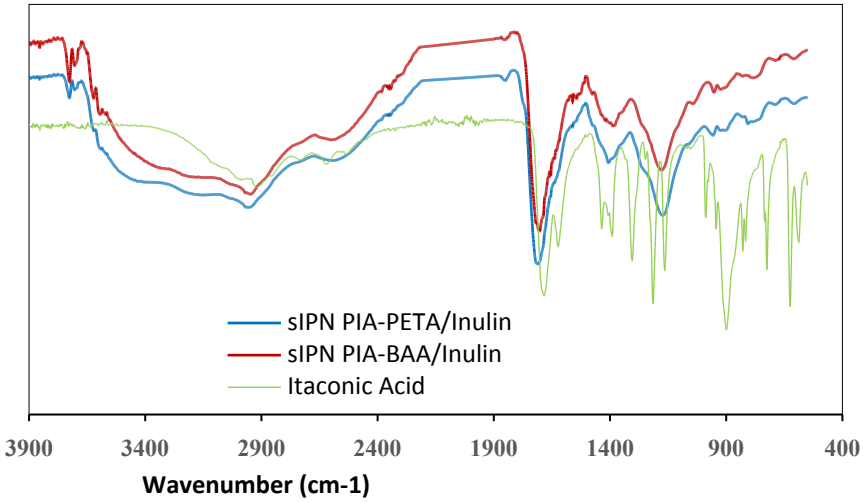

Figure S7. ATR-FTIR spectra of itaconic acid, semi-IPN poly(IA-co-PETA)/inulin and semi-IPN poly(IA-co-BAA)/inulin

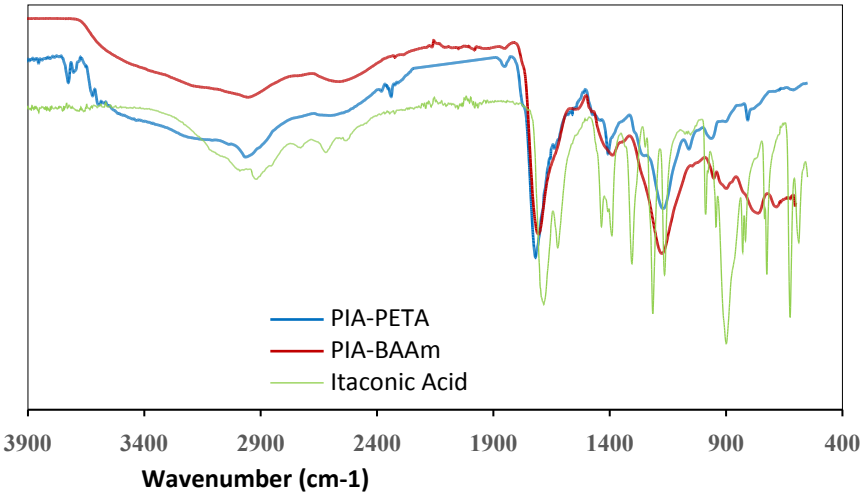

Figure S8. ATR-FTIR spectra of itaconic acid, poly(IA-co-PETA) and poly(IA-co-BAA), both synthesized in Gly-ChCl DES.

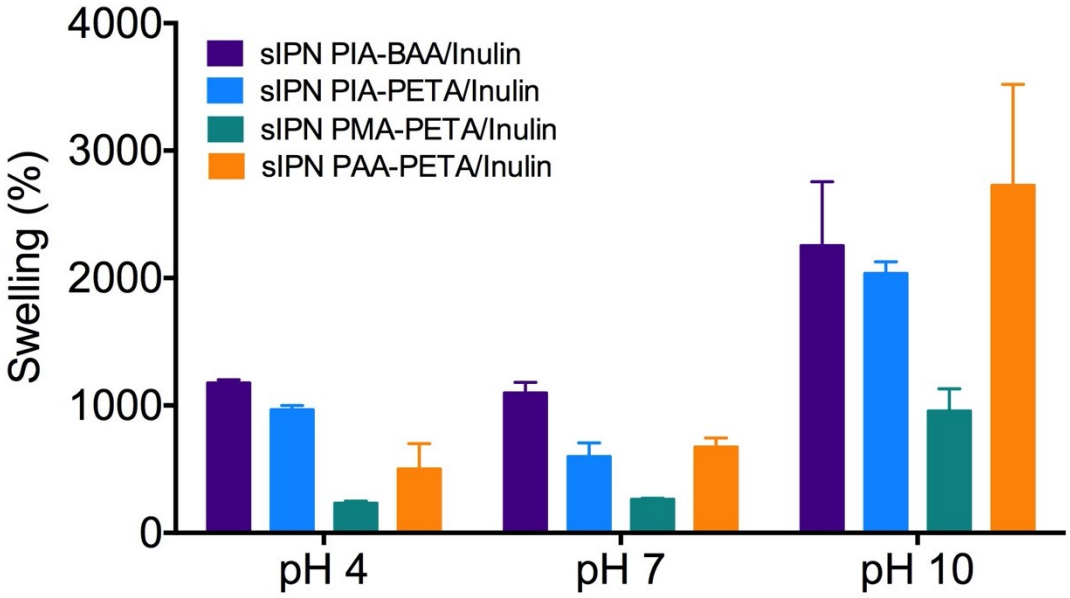

Figure S9. Swelling behavior of semi-IPNs: poly(IA-co-PETA)/inulin, poly(IA-co-BAA)/inulin, poly(acrylic acid-co-PETA)/inulin and poly(methacrylic acid-co-PETA)/inulin, at different pH.

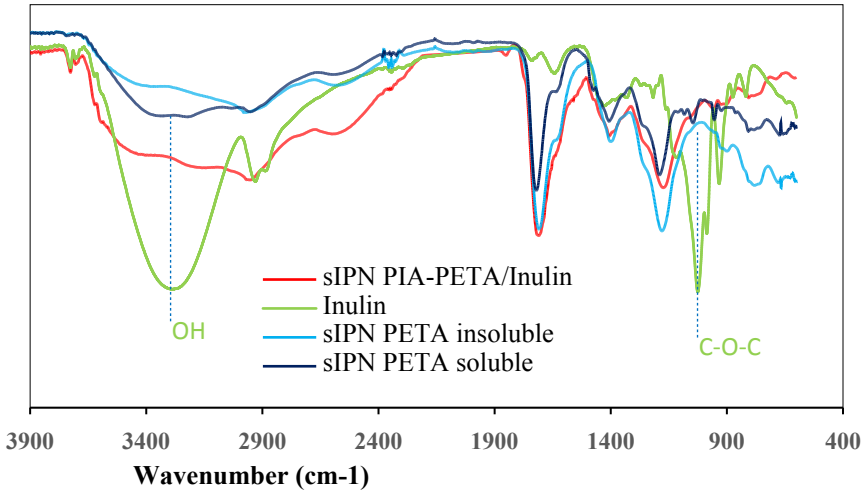

Figure S10. ATR-FTIR spectra of insoluble and soluble residues of poly(IA-co-PETA)/Inulin after 6 months at 37°C and pH=1.

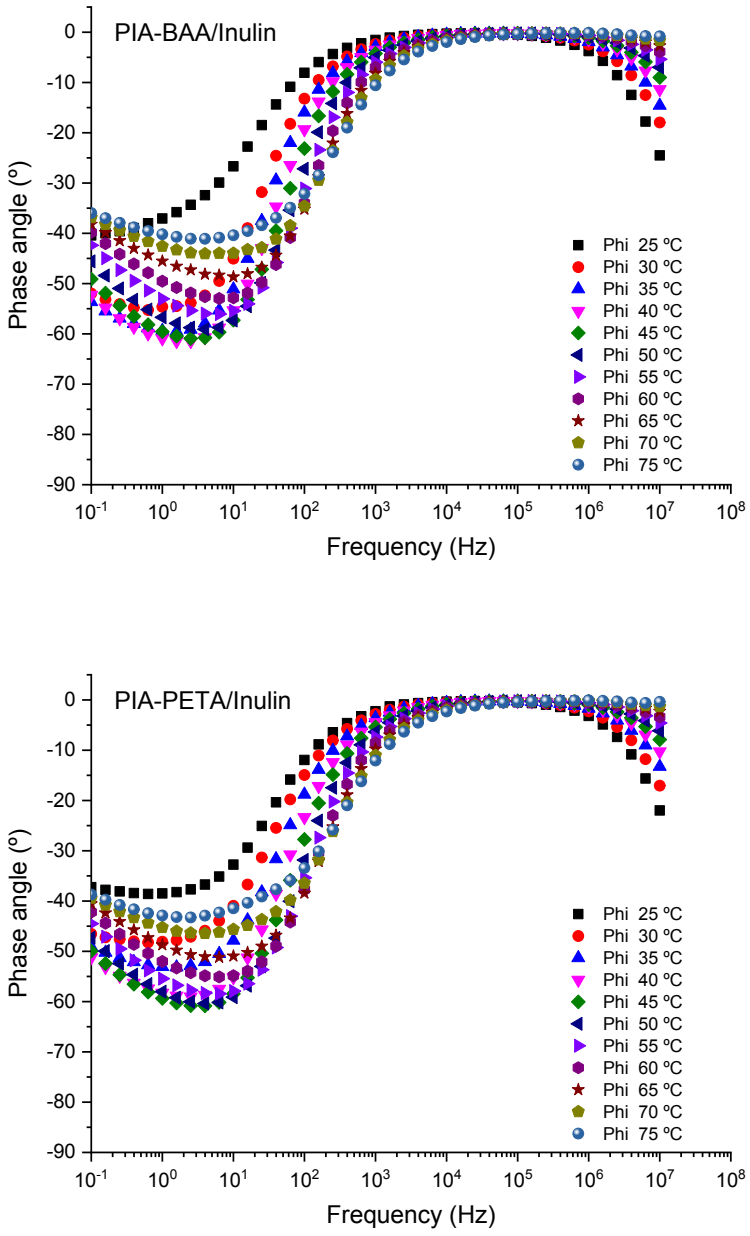

Figure S11. Phase angle versus frequency for the semi-IPNs: PIA-BAA/Inulin (Top) and PIA-PETA/Inulin (Bottom) at different temperatures, both containing Gly-ChCl DES.

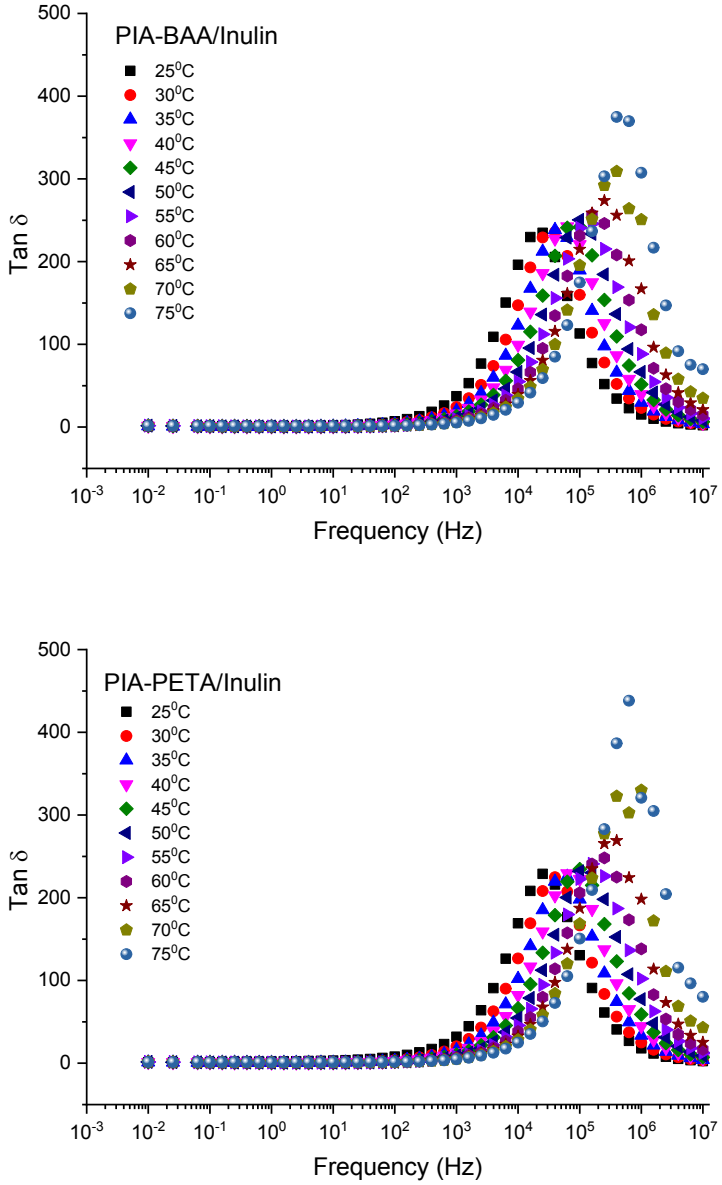

Figure S12. Tan δ versus frequency in all the range of temperatures studied for the semi-IPNs containing Gly-ChCl DES, PIA-BAA/Inulin (Top) and PIA-PETA/Inulin (Bottom).

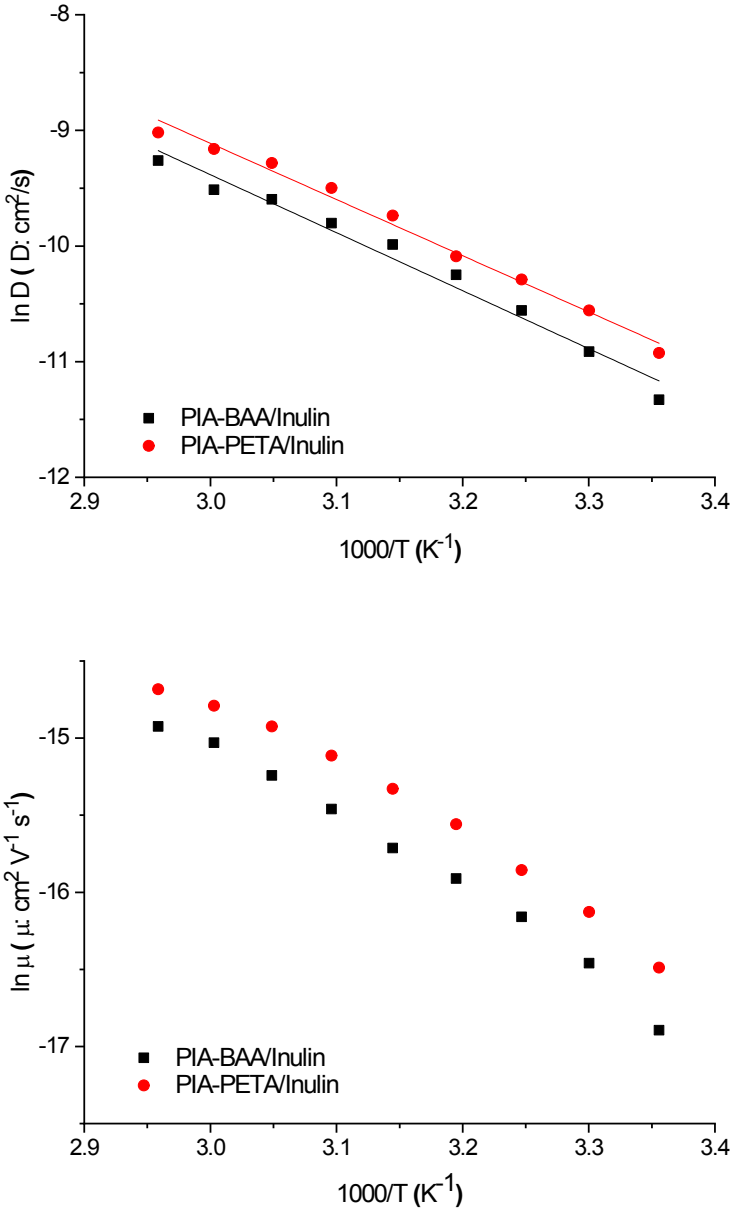

Figure S13. Temperature dependence of diffusivity (Top) and mobility (Bottom) for the ions in the semi-IPNs containing Gly-ChCl DES, PIA-BAA/Inulin and PIA-PETA/Inulin.

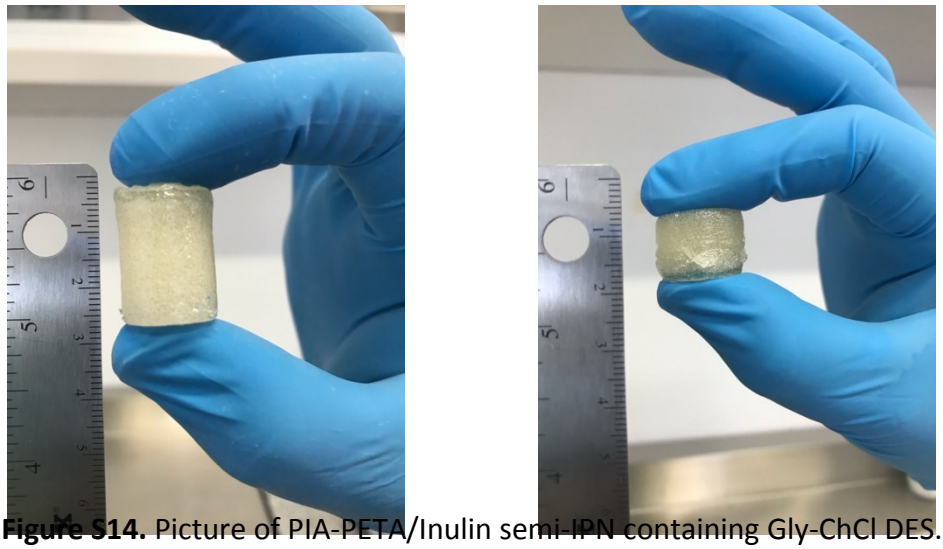

Figure S14. Picture of PIA-PETA/Inulin semi-IPN containing Gly-ChCl DES.